

Simple and modified rule of mixtures of deformation parameters in stage III of single ductile fibre–ductile matrix composites

SHOJIRO OCHIAI, YOTARO MURAKAMI

Department of Metallurgy, Faculty of Engineering, Kyoto University, Kyoto 606, Japan

By employing a single thick molybdenum fibre–copper matrix composite with very weak interfacial bonding, it was confirmed that flow stress, internal stress, effective stress and change in flow stress due to change in strain rate of the composite obey the simple rule of mixtures; strain-hardening exponent, stress exponent of strain rate, effective stress exponent of dislocation velocity and activation volume obey the modified rule of mixtures in the whole range of plastic deformation of the composite. This means that the inherent features of the fibre in the present composite were conserved beyond the failure strain of the fibre tested alone, and the above deformation parameters of the composite were, to a first approximation, determined by the inherent parameters of the fibre and the matrix.

1. Introduction

Macro-scale mechanical properties of composites have been shown to obey the simple rule of mixtures (ROM) [1, 2]. However, the deformation behaviour of composites is essentially connected to dislocation motions in composites, and therefore the dynamic nature of plastic deformation of composites and its relation to thermally activated dislocation mechanisms should be studied.

Recently, we have found that, in stage III-(1) of deformation, ranging from the onset of plastic deformations of fibre to ϵ_{fu} , the failure strain of fibre tested alone, where the constraint effects are due to the difference in Poisson's ratios between the components and those due to suppression of necking in the fibre, the important parameters concerning dislocation motions in composites, such as flow stress, internal stress, effective stress, change in flow stress due to change in strain rate, stress exponent of strain rate, effective stress exponent of dislocation velocity, activation volume and activation enthalpy of composites, are described by the ordinary simple or modified rule of mixtures [3].

In general, the failure strain of ductile fibre–ductile matrix composites, ϵ_{cu} , is larger than ϵ_{fu} i.e. the embedded fibres are able to be elongated

beyond ϵ_{fu} . This means that the necking in fibres is suppressed in composites. In state III-(2), ranging from ϵ_{fu} to ϵ_{cu} , lateral constraints [4] or local strain hardening [5, 6] might arise in composites. To clarify the deformation behaviour in stage III-(2), the aforementioned deformation parameters concerning with dislocation motions are to be needed.

The aims of the present paper are to measure the deformation parameters in stage III-(2) as well as in stage III-(1) and to examine whether or not the parameters in stage III-(2) obey the simple or modified ROM.

The present experiment had two characteristics. First, the specimens used in this work, prepared by the electro-plating method, had a very weak fibre/matrix interface. Therefore, the constraint effect of the matrix on the necking of fibre due to interfacial bonding [4] need not enter the discussion. Second, the specimens were composed of a single thick fibre and surrounding matrix. Therefore, small-fibre strengthening of the matrix [7, 8] could be precluded, and also the effects of neighbouring fibres [4, 9] eliminated.

2. Experimental procedure

The fibre and matrix employed were commercially

pure molybdenum wire of 500 μm diameter and pure copper, respectively. First the fibre was boiled for 600 sec in a saturated sodium hydroxide solution to remove graphite lubricants and oxides, and then rinsed in water. The single fibre composite specimens were prepared by electrolytically plating copper on to the fibre. The solution and operating conditions for plating are described elsewhere [5]. The volume fraction of fibre, V_f , was varied by changing the thickness of the copper layer. Some specimens were annealed at 873° K for 1.8×10^3 sec (type A specimen). The Mo–Cu interface was very weak as shown later. To reduce the interfacial strength further, most specimens were thermally cycled 100 times between 273 and 573 K [10], and then annealed at 873 K for 1.8×10^3 sec (type TA specimen). The difference in interfacial strength between type A and TA specimens was clearly found by the pull-out test, as shown later.

Tensile tests were conducted with an Instron-type tensile testing machine at room temperature mainly employing type TA specimens. Flow stress and strain-hardening exponent were measured by a simple tensile test. The internal stress was measured by an incremental unloading test [11], and then the effective stress was calculated by subtracting the internal stress from flow stress. The change in flow stress due to the change in strain rate was measured by the strain-rate cycling test. The stress exponent of strain rate, effective stress exponent of dislocation velocity and activation volume were measured by the differential tests [12]. A simple tensile test was made by straining specimens at a strain rate of $4.2 \times 10^{-4} \text{ sec}^{-1}$. In incremental unloading to measure the internal stress, specimens were first strained at $4.2 \times 10^{-4} \text{ sec}^{-1}$ strain rate

up to some pre-determined strain and the load was incrementally unloaded for 300 sec with a step of 3 N until negative relaxation was observed. The strain-rate cycling test was performed by increasing the strain rate by a factor of 10 and subsequently decreasing the strain rate by the same factor, where the base strain rate was $4.2 \times 10^{-4} \text{ sec}^{-1}$.

3. Results

3.1. Interfacial strength

At first copper was plated on to polished surfaces of bulk molybdenum and then the tensile strength of the Mo–Cu interface was measured. It was nearly zero similar to that of W/Cu composite prepared by the same method [10, 13]. The shear strength of the interface of W/Cu composites measured by the pull-out test [2, 10] was also very weak (but not zero). The result of pull-out tests of the present composite are presented in Fig. 1 which shows the stress in the fibre at pull-out (open points) or fibre fracture (filled points) as a function of the embedded length, l , divided by the diameter, d . From this result, the interfacial shear strength was calculated to be 17 and 6.4 MPa for type A and TA specimens, respectively. It is evident that thermal-cycling treatment reduced further the originally very low interfacial strength. The reason why the shear strength of the interface was not zero, although the actual interfacial bonding strength was nearly zero, can be explained by the interlocking effect of the interface [10, 13].

It is reasonable to expect that the very weak interface of the present composite could not inhibit necking in the fibre, i.e. the lateral constraint effect of the matrix on fibre necking through interface [4] could not arise, especially in type TA specimens.

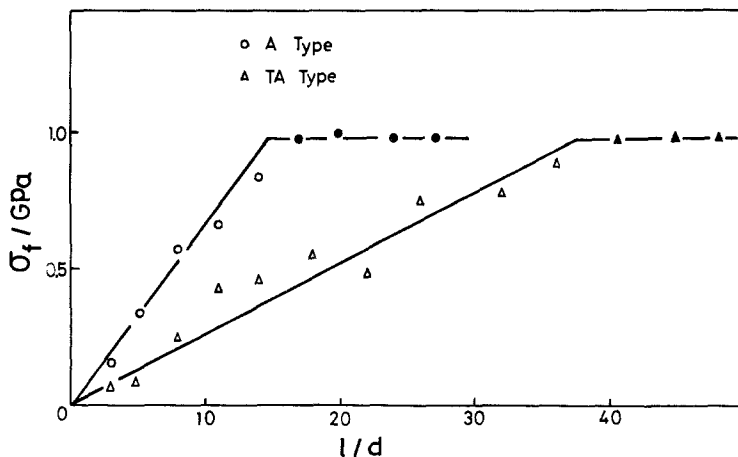


Figure 1 Fibre stress of type A and TA composites at pull-out (open points) or fibre fracture (filled points) as a function of the embedded length, l , divided by the diameter, d .

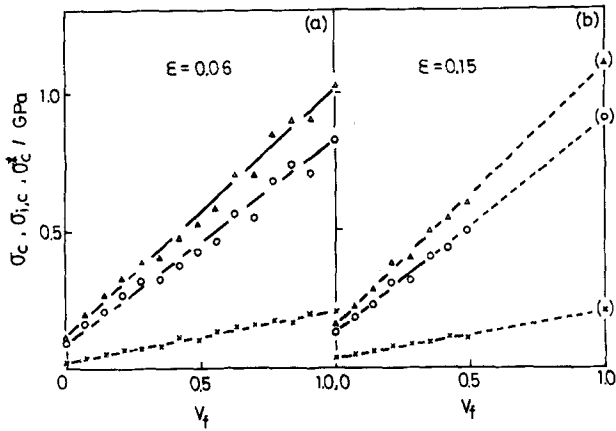


Figure 2 The measured values of $\sigma_c(\Delta)$, $\sigma_{i,c}(0)$ and $\sigma_c^*(x)$ of type TA composite at $\epsilon = 0.06$ and 0.15 versus V_f .

3.2. Flow stress, internal stress, and effective stress

The average value of ϵ_{fu} was 0.08 in true strain, while the failure strain of the matrix was 0.44 on average. The flow stress, σ_c , internal stress $\sigma_{i,c}$ and effective stress σ_c^* of type TA specimens were measured for $\epsilon = 0.06$ and 0.15. The measured values are shown as function of V_f in Fig. 2 where the measured values for $\epsilon = 0.15$ are restricted to the range of $V_f < 0.50$, since the specimens with $V_f > 0.50$ could not be stretched beyond $\epsilon = 0.15$. For $\epsilon = 0.05$, it is evident that all of σ_c , $\sigma_{i,c}$ and σ_c^* obey the simple rule of mixtures given by

$$\sigma_c = \sigma_f V_f + \sigma_m V_m \quad (1)$$

$$\sigma_{i,c} = \sigma_{i,f} V_f + \sigma_{i,m} V_m \quad (2)$$

$$\sigma_c^* = \sigma_f^* V_f + \sigma_m^* V_m, \quad (3)$$

where the subscripts f and m refer to fibre and matrix, respectively. For $\epsilon = 0.15$, these stresses also increase linearly with increasing V_f , indicating

that the rule of mixtures given by Equations 1 to 3 are conserved beyond ϵ_{fu} . The values of σ_f (Δ at $V_f = 1.00$ in Fig. 2), $\sigma_{i,f}(0)$ and $\sigma_f^*(x)$ at $\epsilon = 0.15$ are inferred to be 1.10, 0.90 and 0.20 GPa by extrapolating the measured values to $V_f = 1.00$. These inferred values will be used in Section 4.

3.3. Change in flow stress due to change in strain rate

The change in flow stress of type TA composite due to change in strain rate, $\Delta\sigma_c^{\dot{\epsilon}}$, is shown in Fig. 3 in which $\Delta\sigma_c^{\dot{\epsilon}}/\Delta\ln \dot{\epsilon}$ is plotted against V_f where $\Delta\ln \dot{\epsilon}$ is equal to $\ln(\dot{\epsilon}_2/\dot{\epsilon}_1)$, and $\dot{\epsilon}_1$ and $\dot{\epsilon}_2 (= 10\dot{\epsilon}_1)$ are base and increased strain rates. It is obvious that, for both $\epsilon = 0.06$ and 0.15, $\Delta\sigma_c^{\dot{\epsilon}}$ increases linearly with increasing V_f . The simple rule of mixtures given by

$$\Delta\sigma_c^{\dot{\epsilon}} = \Delta\sigma_f^{\dot{\epsilon}} V_f + \Delta\sigma_m^{\dot{\epsilon}} V_m \quad (4)$$

is valid in both ranges of $\epsilon < \epsilon_{fu}$ and $\epsilon > \epsilon_{fu}$.

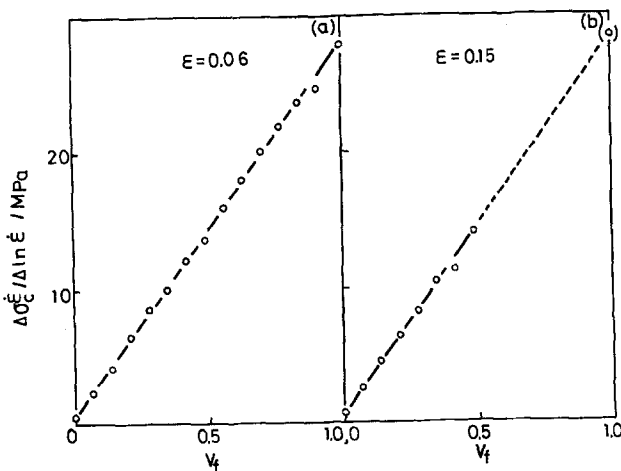


Figure 3 The measured values of $\Delta\sigma_c^{\dot{\epsilon}}/\Delta\ln \dot{\epsilon}$ of type TA composite at $\epsilon = 0.05$ and 0.15 versus V_f .

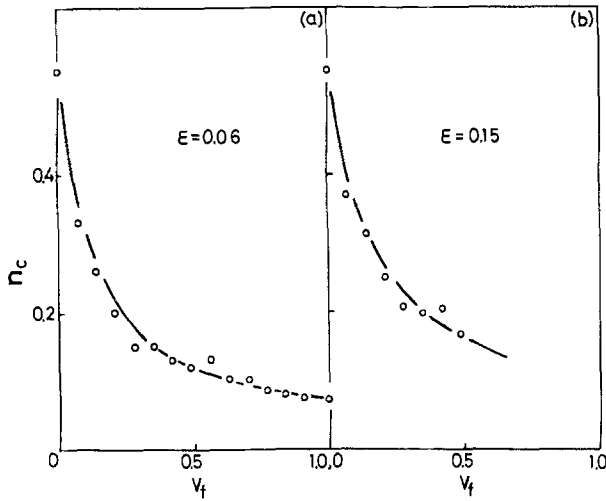


Figure 4 The measured values of n_c of type TA composite at $\epsilon = 0.06$ and 0.15 versus V_f .

3.4. Strain-hardening exponent

The strain-hardening exponent, n_c , of the composite is given by

$$n_c = \frac{\partial \ln \sigma_c}{\partial \ln \epsilon} \quad (5)$$

Experimentally, we obtained the values of n_c at $\epsilon = 0.06$ and 0.15 by employing the equations

$$n_c(\epsilon = 0.06) = \frac{\ln\{\sigma_c(\epsilon = 0.07)/\sigma_c(\epsilon = 0.05)\}}{\ln(0.07/0.05)}$$

and

$$n_c(\epsilon = 0.15) = \frac{\ln\{\sigma_c(\epsilon = 0.16)/\sigma_c(\epsilon = 0.14)\}}{\ln(0.16/0.14)}$$

The measured values of n_c of type TA specimens does not obey the simple ROM as shown in Fig. 4.

3.5. Stress exponent of strain rate and effective stress exponent of dislocation velocity

The stress exponent of strain rate, m , and the effective stress exponent of dislocation velocity, m^* , are respectively given by

$$m = \frac{\partial \ln \dot{\epsilon}}{\partial \ln \sigma} \quad (6)$$

$$m^* = \frac{\partial \ln \dot{\epsilon}}{\partial \ln \sigma^*} \quad (7)$$

Assuming that internal stress does not change at a given strain during the strain rate cycling test, we obtained these parameters of TA specimens (m_c and m_c^*) by employing the equations $m_c = \ln(\dot{\epsilon}_2/\dot{\epsilon}_1)/\ln((\sigma_c + \Delta\sigma_c^{\dot{\epsilon}})/\sigma_c)$ and $m_c^* = \ln(\dot{\epsilon}_2/\dot{\epsilon}_1)/\ln((\sigma_c^* + \Delta\sigma_c^{\dot{\epsilon}})/\sigma_c^*)$. Figs. 5 and 6 show the measured values of m_c and m_c^* at $\epsilon = 0.06$ and 0.15 as a function of V_f .

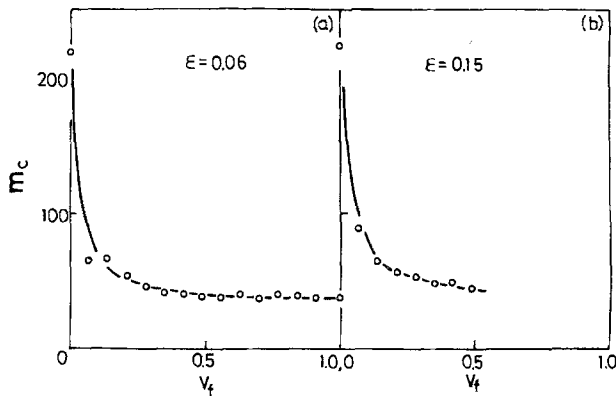


Figure 5 The measured values of m_c of type TA composite at $\epsilon = 0.05$ and 0.15 versus V_f .

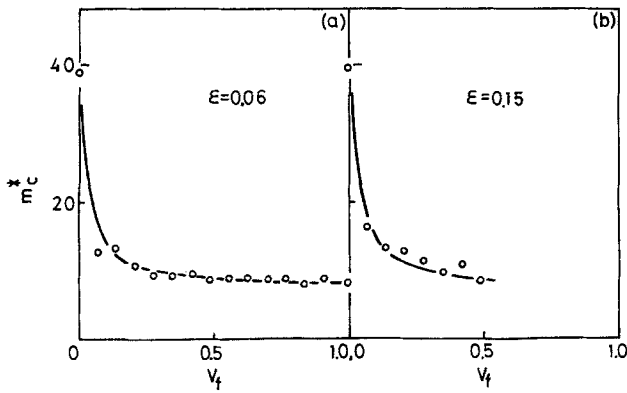


Figure 6 The measured values of m_c^* of type TA composite at $\epsilon = 0.06$ and 0.15 versus V_f .

3.6. Activation volume

The activation volume V^* is given by

$$V^* = M k T \frac{\partial \ln \dot{\epsilon}}{\partial \sigma \dot{\epsilon}}, \quad (8)$$

where M is the Taylor factor, k Boltzmann's constant, and T the temperature. In this work, the Taylor factors of fibre (M_f) and matrix (M_m) were assumed to be 2.75 and 3.06, respectively, and that of composite (M_c) was, to a first approximation, calculated by employing the equation [3]

$$M_c = M_f V_f + M_m V_m. \quad (9)$$

Substituting the measured values of $\Delta \ln \dot{\epsilon} / \Delta \sigma \dot{\epsilon}$ of type TA specimens and the values of M_c inferred from Equation 9 into $V_c^* = M_c k T \Delta \ln \dot{\epsilon} / \Delta \sigma \dot{\epsilon}$, we have the $V_c^* - V_f$ relation for $\epsilon = 0.06$ and 0.15 as shown in Fig. 7.

4. Discussion

In Sections 3.1 and 3.2, it was clarified that σ_c , σ_c^* and $\Delta \sigma \dot{\epsilon}$ obey the simple ROM in both

ranges of $\epsilon < \epsilon_{fu}$ and $\epsilon > \epsilon_{fu}$. In this section, we would like to examine whether n_c , m_c , m_c^* and V_c^* obey the modified rule of mixtures both for $\epsilon < \epsilon_{fu}$ and $\epsilon > \epsilon_{fu}$ or not.

First we take the case of n_c . As the fibre and matrix are subjected to the same axial strain, by substituting Equation 1, $n_f = \partial \ln \sigma_f / \partial \ln \epsilon$, and $n_m = \partial \ln \sigma_m / \partial \ln \epsilon$ into Equation 5, we have

$$n_c = n_f \cdot \frac{\sigma_f V_f}{\sigma_f V_f + \sigma_m V_m} + n_m \cdot \frac{\sigma_m V_m}{\sigma_f V_f + \sigma_m V_m} \quad (10)$$

putting

$$\alpha = \sigma_f V_f / (\sigma_f V_f + \sigma_m V_m) \quad (11)$$

we have

$$n_c = n_f \cdot \alpha + n_m \cdot (1 - \alpha). \quad (12)$$

Equation 12 may be regarded as a modified rule of mixtures for n_c . Substituting the measured values of σ_f and σ_m at $\epsilon = 0.06$, and the measured value of σ_m and the inferred value of σ_f (Fig. 2) at $\epsilon = 0.15$ into Equation 11, and plotting the measured

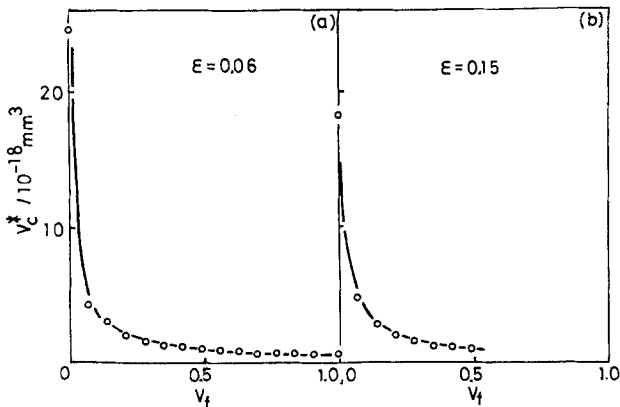


Figure 7 The measured values of V_c^* of type TA composite at $\epsilon = 0.06$ and 0.15 versus V_f .

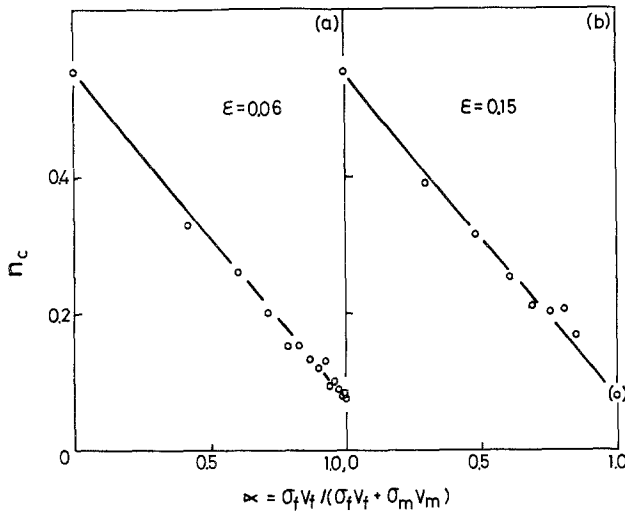


Figure 8 The measured values of n_c of type TA composite at $\epsilon = 0.06$ and 0.15 plotted against $\alpha = \sigma_f V_f / (\sigma_f V_f + \sigma_m V_m)$.

values of n_c against α , we have n_c - α relations for $\epsilon = 0.06$ and 0.15 as shown in Fig. 8. The values of n_c at both $\epsilon = 0.06$ and 0.15 decrease linearly with increasing α . This strongly suggests that n_c obeys the modified ROM given by Equation 12 for both $\epsilon < \epsilon_{fu}$ and $\epsilon > \epsilon_{fu}$. Extrapolating the n_c - α relation at $\epsilon = 0.15$ to $V_f = 1.00$ we have $n_f = 0.08$. This value is the same as 0.08 of n_f at $\epsilon = 0.06$. The values of n_m at $\epsilon = 0.06$ and 0.15 are also the same. This indicates that the value of n_f and n_m remain nearly constant in the strain range investigated.

In the previous paper [3], we have already shown that, in the deformation stage III-(1) ($\epsilon < \epsilon_{fu}$), the modified ROMs of m_c , m_c^* and V_c^* are given by

$$\frac{1}{m_c} = \frac{\alpha}{m_f} + \frac{1-\alpha}{m_m}, \alpha = \sigma_f V_f / (\sigma_f V_f + \sigma_m V_m) \quad (13)$$

$$\frac{1}{m_c^*} = \frac{\alpha}{m_f^*} + \frac{1-\alpha}{m_m^*}, \alpha = \sigma_f^* V_f / (\sigma_f^* V_f + \sigma_m^* V_m) \quad (14)$$

$$\frac{1}{V_c^*} = \frac{\alpha}{V_f^*} + \frac{1-\alpha}{V_m^*}, \alpha = M_f V_f / (M_f V_f + M_m V_m). \quad (15)$$

Plotting $1/m_c$ against $\alpha = \sigma_f V_f / (\sigma_f V_f + \sigma_m V_m)$ for $\epsilon = 0.06$ and 0.15 , we have the linear relation between $1/m_c$ and α , as shown in Fig. 9. This result strongly suggests that the modified ROM given by Equation 13 is valid not only for $\epsilon < \epsilon_{fu}$ but also for $\epsilon > \epsilon_{fu}$. Similarly, plotting $1/m_c^*$ and $1/V_c^*$ against $\alpha = \sigma_f^* V_f / (\sigma_f^* V_f + \sigma_m^* V_m)$ and $\alpha = M_f V_f / (M_f V_f + M_m V_m)$, respectively, we can see the linear relations between $1/m_c^*$ and α and between $1/V_c^*$ and α , for both $\epsilon < \epsilon_{fu}$ and $\epsilon > \epsilon_{fu}$, as shown in Figs. 10 and 11.

It is clear that n_c , m_c , m_c^* and V_c^* obey the modified ROMs not only for $\epsilon < \epsilon_{fu}$ but also for $\epsilon > \epsilon_{fu}$. It is important that m_f^* and V_f^* are independent of ϵ , since the extrapolated values of m_f^* in Fig. 10 and V_f^* in Fig. 11 at $\epsilon = 0.15$ are the same as those at $\epsilon = 0.06$. This is a feature of b c c metals because the mechanism controlling the deformation of b c c metals is concerned with

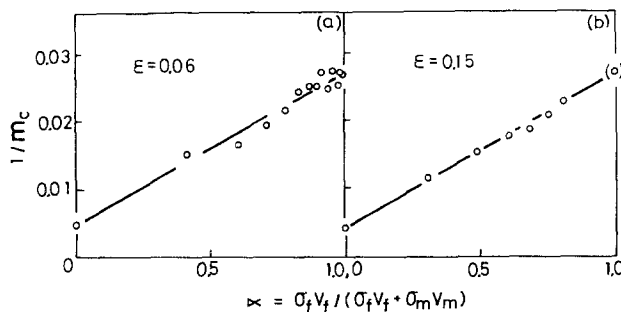


Figure 9 The measured values of $1/m_c$ of type TA composite at $\epsilon = 0.06$ and 0.15 plotted against $\alpha = \sigma_f V_f / (\sigma_f V_f + \sigma_m V_m)$.

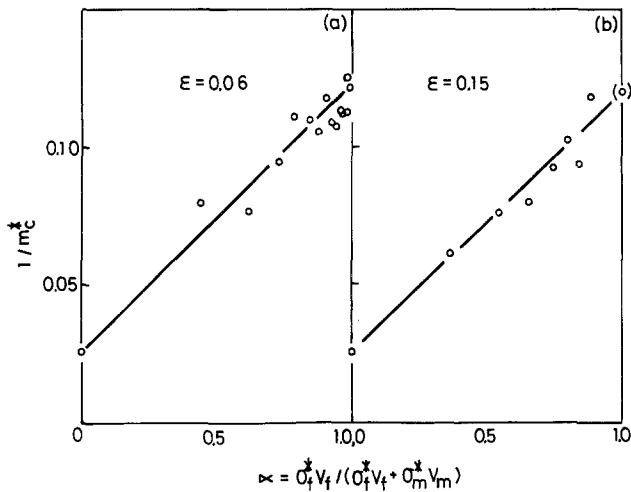


Figure 10 The measured values of $1/m_c^*$ of type TA composite at $\epsilon = 0.06$ and 0.15 plotted against $\alpha = \sigma_f^*V_f / (\sigma_f^*V_f + \sigma_m^*V_m)$.

overcoming the Peierls–Nabarro stress which is independent of ϵ [12]. These results imply that inherent features of the fibre in the present composites are conserved beyond ϵ_{fu} , and the deformation parameters are determined by the inherent parameters of the fibre and the matrix.

When the fibre is firmly bonded to the matrix, the necking in the fibre will be prevented from developing by the matrix, through the positive radial and hoop stresses [4]. For such a case, these stresses might lead the deformation parameters not obeying the simple and modified ROMs. On the other hand, when the interface is weak, as in the present composite, such stresses would be negligible. This might be the reason why the parameters obey the ROMs in the present composite.

The fibres in the present composite, for $\epsilon > \epsilon_{fu}$, exhibited apparently uniform elongation but not multiple necking. This is also the reason why the parameters obey the ROMs at the point where V_f

does not vary along the length during deformation. The reason why the fibre in the weakly bonded composite is able to be stretched apparently uniformly and the stability of such a composite, will be studied in the following paper.

5. Conclusions

By employing a single thick molybdenum fibre–copper matrix composite with very weak interfacial bonding, deformation parameters such as flow stress, internal stress, effective stress, change in flow stress due to change in strain rate, strain–hardening exponent, stress exponent of strain rate, effective stress exponent of dislocation velocity and activation volume, were measured. The inherent features of the fibre in the present composite were conserved beyond the failure strain of the fibre tested alone. The above deformation parameters, to a first approximation, obey the simple or modified rule of mixtures, which were

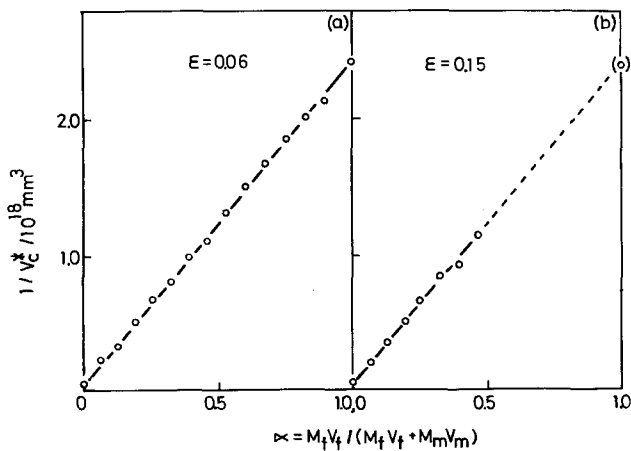


Figure 11 The measured values of $1/V_c^*$ of type TA composite at $\epsilon = 0.06$ and 0.15 plotted against $\alpha = M_fV_f / (M_fV_f + M_mV_m)$.

composed of the inherent parameters of the fibre and the matrix.

References

1. D. L. MCDANELS, R. W. JECH and J. W. WEETON, *Trans. Met. Soc. AIME* **233** (1965) 636.
2. A. KELLY and W. R. TYSON, *J. Mech. Phys. Solids* **13** (1965) 329.
3. S. OCHIAI and Y. MURAKAMI, *J. Mater. Sci.* **14** (1979) 1187.
4. H. R. PIEHLER, *Trans. Met. Soc. AIME* **233** (1965) 12.
5. S. OCHIAI, K. SHIMOMURA and Y. MURAKAMI, *Met. Sci.* **9** (1975) 535.
6. R. M. VENNETT, S. M. VOLF and A. P. LEVITT, *Met. Trans.* **1** (1970) 1569.
7. G. GARMONG and L. A. SHEPARD, *ibid.* **2** (1971) 175.
8. A. KELLY and H. LILHOLT, *Phil. Mag.* **20** (1969) 311.
9. K. NAKAZAWA and S. UMEKAWA, *J. Japan Inst. Metals* **36** (1972) 398.
10. S. OCHIAI, S. OKUDA, K. SHIMOMURA and Y. MURAKAMI, *Trans. Jap. Inst. Metals* **10** (1976) 649.
11. S. R. MACEVEN, O. A. KUPCIS and B. RAMASWAMI, *Scripta Met.* **3** (1969) 441.
12. H. CONRAD, *J. Metals* **16** (1964) 582.
13. G. A. COOPER, *J. Mater. Sci.* **2** (1967) 409.

Received 13 June and accepted 20 November 1979.